mGluR5 stimulates gliotransmission in the nucleus accumbens

Marcello D'Ascenzo*†‡, Tommaso Fellin*†, Miho Terunuma†, Raquel Revilla-Sanchez†, David F. Meaney§, Yves P. Auberson¶, Stephen J. Moss†, and Philip G. Haydon*†‖

*Silvio Conte Center for Integration at the Tripartite Synapse, †Department of Neuroscience, University of Pennsylvania School of Medicine, Philadelphia, PA 19104; ‡Institute of Human Physiology, Catholic University, Largo Francesco Vito 1, 00168 Roma, Italy; §Department of Bioengineering, University of Pennsylvania, 3320 Smith Walk, Hayden Hall, Philadelphia, PA 19104; and ¶Novartis Institutes for BioMedical Research, Novartis Pharma AG, Klybeckstrasse 141, CH-4002 Basel, Switzerland

Edited by Susan G. Amara, University of Pittsburgh School of Medicine, Pittsburgh, PA, and approved November 29, 2006 (received for review October 24, 2006)

Although metabotropic glutamate receptor 5 (mGluR5) is essential for cocaine self-administration and drug-seeking behavior, there is limited knowledge of the cellular actions of this receptor in the nucleus accumbens (NAc). Although mGluR5 has the potential to regulate neurons directly, recent studies have shown the importance of mGluR5 in regulating Ca^{2+} signaling in astrocytes and, as a consequence, the Ca^{2+}-dependent release of excitatory transmitters from these glia. In this study, we demonstrate that activation of mGluR5 induces Ca^{2+} oscillations in NAc astrocytes with the correlated appearance of NMDA receptor-dependent slow inward currents detected in medium spiny neurons (MSNs). Photolysis of caged Ca^{2+} loaded specifically into astrocytes evoked slow inward currents demonstrating that Ca^{2+} elevations in astrocytes are responsible for these excitatory events. Pharmacological evaluation of these glial-evoked NMDA currents shows that they are mediated by NR2B-containing NMDA receptors, whereas synaptic NMDA receptors rely on NR2A-containing receptors. Stimulation of glutamatergic afferents activates mGluR5-dependent astrocytic Ca^{2+} oscillations and gliotransmission that is sustained for minutes beyond the initial stimulus. Because gliotransmission is mediated by NMDA receptors, depolarized membrane potentials exhibited during up-states augment excitation provided by gliotransmission, which drives bursts of MSN action potentials. Because the predominant mGluR5-dependent action of glutamatergic afferents is to cause the sustained activation of astrocytes, which in turn excite MSNs through extrasynaptic NMDA receptors, our results raise the potential for gliotransmission being involved in prolonged mGluR5-dependent adaptation in the NAc.

addiction | astrocytes | glutamate release | NMDA receptors

Although the dopaminergic system is known to play important roles in responses to drugs of abuse, there is an increasing awareness of the importance of glutamate in mediating effects of these drugs in the brain (1). Cocaine administration requires glutamatergic transmission in the nucleus accumbens (NAc) for drug-seeking behavior (2, 3) with accumulating evidence demonstrating the importance of metabotropic glutamate receptors (mGluRs) in mediating the actions of extracellular glutamate after cocaine use (4). mGluR5 knockout mice do not acquire cocaine self-administration behavior (4), and in wild-type mice the mGluR5 antagonist, 2-methyl-6-(phenylethynyl)pyridine hydrochloride (MPEP), decreases cocaine, morphine, and nicotine self-administration and drug-seeking behavior (5–8).

Although astrocytes are electrically inexcitable, emerging evidence demonstrates that these nonneuronal cells respond to neurotransmitters with elevations in their internal Ca^{2+} and with the release of the chemical transmitters glutamate, ATP and D-serine (9, 10). Because astrocytes and neurons release common chemical transmitters, we use the term gliotransmitter and gliotransmission to refer to their release from astrocytes (11). Recent molecular genetic manipulation of astrocytes has shown that through the release of gliotransmitters, astrocytes can coordinate synaptic networks in the hippocampus (12). Moreover, several lines of evidence show that astrocytes express class I mGluRs, in particular mGluR5 (13–15), which when activated can induce gliotransmission (15).

Class I mGluRs are critical for gliotransmission in the hippocampus and cortex; however, there is little information concerning this receptor system in glial cells elsewhere in the nervous system. Drugs of abuse have convergent actions in the NAc suggesting that this is an important brain region mediating rewarding properties (16, 17). Because of the powerful excitation provided by astrocytes to pyramidal neurons in the hippocampus (18, 19), and because mGluR5 is critical for drug-seeking behavior (4), we have asked whether mGluR5-dependent gliotransmission regulates medium spiny neuron (MSN) excitability in the NAc and thus whether gliotransmission has the potential to provide an excitatory signal underlying the reward pathway that is centered in the NAc.

Results

mGluR5-Dependent Ca^{2+} Signaling in Astrocytes. We used brain slices from pGFAP-GFP mice, in which the glial fibrillary acidic protein promoter drives the expression of GFP (20) for fluorescence-guided patch-clamping. GFP fluorescent cells have small (<10 μm) somata with highly ramified processes (Fig. 1*A*). Action potentials were never evoked when currents were injected in current-clamp mode into GFP-expressing cells (Fig. 1*B*; $n = 15$), and they displayed a more negative resting potential than MSNs [-89.7 ± 1.4 mV, $n = 15$; see supporting information (SI) Table 1]. GFP-expressing cells have a linear current/voltage relationship (Fig. 1*C*), typical of passive astrocytes in other brain regions (21, 22) with an input resistance of 17.8 ± 3.0 MΩ ($n = 15$). To assess whether the GFP-positive cells in the NAc are gap junction-coupled, we performed paired recording from two GFP-positive cells. Depolarization caused bidirectional current flow between paired cells ($n = 3$ pairs; Fig. 1*D*). When Alexa 568 was included in pipette solution, dye coupling was detected in adjacent GFP-labeled cells (SI Fig. 6).

Although it is known that MSNs express mGluR5, it is unknown whether astrocytes express this group I metabotropic receptor. The expression of mGluR5 in the NAc was confirmed by using Western

Author contributions: M.D. and T.F. contributed equally to this work; M.D., T.F., and P.G.H. designed research; M.D., T.F., M.T., and R.R.-S. performed research; D.F.M., Y.P.A., and S.J.M. contributed new reagents/analytic tools; M.D. and T.F. analyzed data; and M.D., T.F., and P.G.H. wrote the paper.

Conflict of interest statement: P.G.H. has equity interest in the company Prairie Technologies, Inc., which manufactures the two-photon microscope used in this study.

This article is a PNAS direct submission.

Abbreviations: ACSF, artificial cerebrospinal fluid; AMPA, α-amino-3-hydroxy-5-methyl-4-isoxazolepropionic acid; DHPG, (*RS*)-3,5-dihydroxyphenylglycine; EPSC, excitatory postsynaptic current; EPSP, excitatory postsynaptic potential; MPEP, 2-methyl-6-(phenylethynyl)pyridine hydrochloride; MSN, medium spiny neuron; NAc, nucleus accumbens; NBQX, 2,3-dioxo-6-nitro-1,2,3,4-tetrahydrobenzo[*f*]quinoxaline-7-sulfonamide; SIC, slow inward current; TTX, tetrodotoxin.

‖To whom correspondence should be addressed. E-mail: pghaydon@mail.med.upenn.edu.

This article contains supporting information online at www.pnas.org/cgi/content/full/0609408104/DC1.

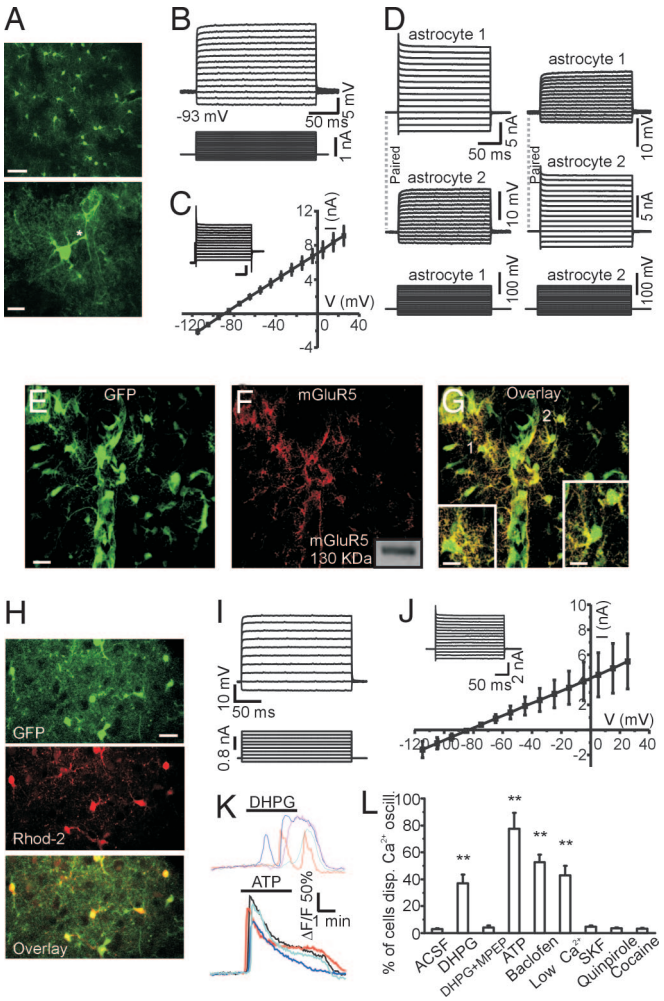

Fig. 1. NAc astrocytes are electrically inexcitable, are electrotonically coupled with one another, express mGluR5 receptors, and respond to neurotransmitters with Ca^{2+} oscillations. (*A*) Two-photon laser-scanning image of GFP-expressing cells from a NAc slice obtained from pGFAP-GFP transgenic mice (*z*-projection of 15 planes). (Scale bar: *Upper*, 40 μm; *Lower*, 10 μm.) An astrocytic endfoot making contact with a capillary (*). (*B*) Typical response of a NAc pGFAP-GFP$^+$ cell to current injections from −0.2 to 1.1 nA (bottom traces, 0.1-nA increments). (*C*) Average whole-cell *I–V* relationship from GFP-expressing cells (n = 15 cells). (*Inset*) Inward and outward currents recorded in voltage-clamp configurations (−135 to +25 mV, 10-mV increments). (Scale bars: 2 nA, 50 ms.) (*D*) Paired recordings from two GFP-positive cells showing bidirectional coupling. (*E–G*) mGluR5 is expressed in NAc astrocytes. Top-view reconstruction obtained from confocal *z*-series of GFP-expressing astrocytes (*E*, green). mGluR5 immunoreactivity (*F*, red) associated with GFP-positive astrocytic processes reveals localization of this receptor mainly in astrocytic processes rather than in astrocytic cell bodies (*G*). [Note that we used an image mask based on the GFP fluorescence of the astrocyte to display pixels displaying mGluR5 immunoreactivity associated with astrocytes (see *SI Materials and Methods*).] *Insets* in *G* show regions 1 and 2 at higher magnification. (Scale bars: *E–G*, 20 μm; *G Inset*, 10 μm.) (*F Inset*) Western blot analysis from isolated NAc slices confirm the presence of the mGluR5 in this brain region . (*H*) NAc slices from pGFAP-GFP mice loaded with Rhod-2 (red) showing selective labeling of GFP expressing astrocytes (green). (Scale bar: 20 μm.) (*I*) Current-clamp recordings from a dye-loaded cell showing astrocytic membrane properties and no action potential firing. (*J*) Average whole-cell *I–V* relationship from dye-loaded cells (n = 3 cells) and representative currents after voltage steps from −115 mV to +25 mV (*Inset*). (*K*) Astrocyte responses (time course of the $\Delta F/F$ ratio) to DHPG (20 μM; *Upper*) and ATP (100 μM; *Lower*). (*L*) Average percentage of astrocytes displaying Ca^{2+} oscillations under the different experimental conditions: ACSF, n = 23 slices; DHPG (20 μM), n = 4 slices; DHPG (20 μM) + MPEP (50 μM), n = 4 slices; ATP (50/100 μM), n = 5 slices; baclofen (40 μM), n = 4 slices; low Ca^{2+}, n = 5 slices; SKF 38393 (2.5–5 μM), n = 3 slices; quinpirole (20 μM), n = 3 slices; and cocaine (1–10 μM), n = 4 slices.

blot analysis and immunocytochemistry (Fig. 1 *E–G*). mGluR5 immunoreactivity was widespread throughout the NAc, consistent with both neuronal and glial labeling (data not shown). To ask whether astrocytes express this receptor, we performed immunocytochemistry in GFAP-GFP transgenic mice and used the presence of GFP expression in astrocytes to make an image mask (see *SI Materials and Methods*) to ask whether mGluR5 immunoreactivity was associated with astrocytic processes. mGluR5 immunoreactivity colocalized with GFP-expressing astrocytic processes and to a lesser extent with the astrocytic cell body and the endfeet that contact the vasculature (Fig. 1 *E–G*).

To investigate Ca^{2+} excitability, slices from pGFAP-GFP mice (20) were incubated with the red-shifted Ca^{2+} indicator Rhod-2 AM. Bulk loaded Ca^{2+} indicator selectively accumulated in GFP-expressing astrocytes (Fig. 1*H*), which display the typical passive properties of NAc astrocytes (Fig. 1 *I* and *J*). Although spontaneous Ca^{2+} oscillations within NAc astrocytes are detected infrequently (Fig. 1*L*), application of the class I mGluR agonist (RS)-3,5-dihydroxyphenylglycine (DHPG) (20 μM) resulted in Ca^{2+} transients that were attenuated by the mGluR5 antagonist MPEP (Fig. 1 *K* and *L*). ATP (50 μM) and baclofen (40 μM), a $GABA_B$ agonist, resulted in intracellular Ca^{2+} elevations in astrocytes (Fig. 1 *K* and *L*). In agreement with the properties of cortical and hippocampal astrocytes (23), perfusion of NAc slices with a low extracellular Ca^{2+} artificial cerebrospinal fluid (ACSF) induced astrocytic Ca^{2+} oscillations (Fig. 1*L*). In contrast, astrocytic Ca^{2+} signals (Fig. 1*L*) were not evoked by cocaine (1–10 μM), the dopamine D_1 receptor agonist SKF 38393 (2.5–5 μM), or the dopamine D_2 agonist quinpirole (20 μM).

mGluR5 Induces Ca^{2+}-Dependent Gliotransmission. To ask whether mGluR5-dependent Ca^{2+} signaling induces gliotransmission and excites MSNs, we recorded from MSNs in the virtual absence of extracellular Mg^{2+}, to relieve the Mg^{2+} block of the NMDA receptors, and in tetrodotoxin (TTX) (1 μM), to block action potential-mediated release from glutamatergic inputs. Slow transient inward currents were detected with kinetics significantly slower than excitatory postsynaptic currents (EPSCs) (Fig. 2*B*) but similar to the astrocyte-dependent slow inward currents (SICs) previously recorded in the hippocampus (Fig. 2 *A* and *B* and SI Table 2) (15, 18, 19). Paired whole-cell recordings from closely spaced (<80 μm) MSNs revealed that SICs can occur in two neurons with a high degree of temporal correlation (Fig. 2*C*). In 11 paired recordings, 7 displayed SICs: of 55 SICs, 16 (29.1%) were found to be synchronized within a time window of 200 ms (Fig. 2*D*).

DHPG (20 μM) caused a slow depolarization in a subpopulation (56%) of MSNs and significantly increased the frequency of SICs (n = 15; Fig. 2 *E* and *F*). ATP, baclofen, or low Ca^{2+} ACSF, stimuli that we showed to effectively trigger Ca^{2+} increases in NAc astrocytes (Fig. 1*L*), caused a significant increase in the frequency of SICs in MSNs (Fig. 2*F*). Cocaine, or the D_1 and D_2 receptor agonists SKF 38393 and quinpirole, which did not activate astrocytic Ca^{2+} signaling, did not stimulate SICs (Fig. 2*F*).

To determine whether the slow currents are generated by a Ca^{2+}-dependent gliotransmission, we selectively stimulated single astrocytes using photolysis of the Ca^{2+} cage NP-EGTA. We focused a UV beam (3-μm diameter) to an astrocytic cell body at a distance from dendrites of the recorded MSN. Photolysis evoked a Ca^{2+} elevation in the astrocyte cell body and caused delayed SICs in adjacent neurons (SI Fig. 7 *A* and *B*; n = 5 of 16). This delay results from the time required for propagation of the Ca^{2+} signal from the cell body to the distal processes. When NP-EGTA was omitted, UV photolysis evoked neither an astrocytic Ca^{2+} elevation nor an SIC in the associated pyramidal neuron (n = 5).

NR2B Subunit-Containing NMDA Receptors Are Activated by Gliotransmission. SICs were reversibly attenuated by the specific NMDA receptor antagonist D-AP5 (50–100 μM; SI Fig. 7*D*) and

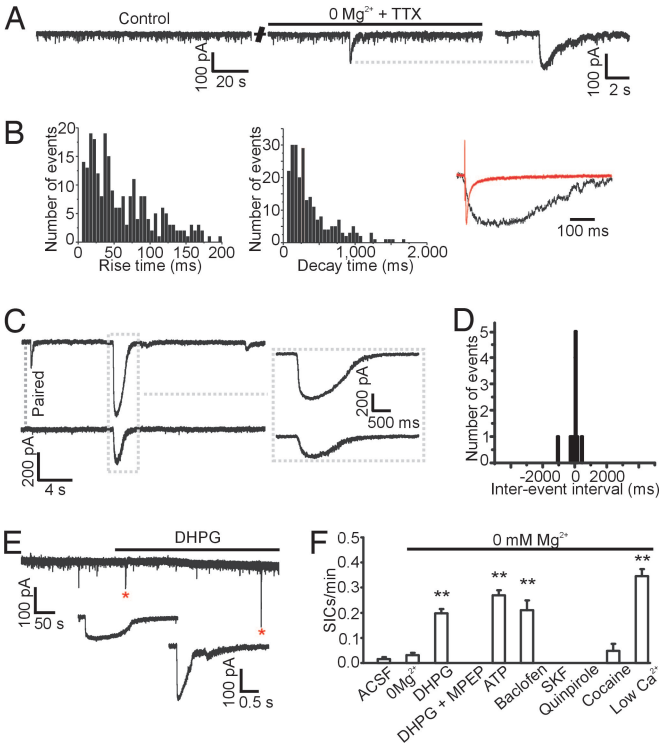

Fig. 2. SICs evoked in MSNs by stimuli that induce astrocytic Ca^{2+} oscillations. (*A*) Patch-clamp recording from an MSN in voltage-clamp showing a spontaneous SIC after slice perfusion with 0 extracellular Mg^{2+} ACSF. Note the slow kinetics typical of SICs compared with miniature postsynaptic currents. V_h = −85 mV. (*B*) Histogram of rise (*Left*; 259 events; bin, 5 ms) and decay (*Center*; 259 events; bin, 50 ms) time of SICs. (*Right*) Overlay of an SIC (black trace) and an EPSC (red trace). (*C*) Representative paired-recording from two MSNs showing synchronous SICs. (*D*) Interevent time interval histogram of SICs occurring in pairs of recorded MSNs (n = 7 pairs). Of a total of 55 SICs, 16 SICs were recorded within a time window of 200 ms. Bins, 50 ms. (*E*) SICs induced by perfusion with DHPG (20 μM); * indicates SIC. (*F*) Average SIC frequency in ACSF, n = 106 cells; 0 mM Mg^{2+}, n = 147 cells; DHPG (20 μM), n = 15 cells; DHPG (20 μM) + MPEP (50 μM), n = 5 cells; ATP (50 μM), n = 9 cells; baclofen (40 μM), n = 6 cells; SKF 38393 (2.5–5 μM), n = 5 cells; quinpirole (20 μM), n = 5 cells; cocaine (1–10 μM), n = 9 cells; and low Ca^{2+}, n = 95 cells.

unaffected by the α-amino-3-hydroxy-5-methyl-4-isoxazolepropionic acid (AMPA)-receptor antagonist 6-cyano-2,3-dihydroxy-7-nitro-quinoxaline disodium salt (CNQX, 25 μM; SI Fig. 7*E*), demonstrating that glutamate release from NAc astrocytes activates NMDA receptor in MSNs. Using NMDA receptor antagonists, we asked whether gliotransmission and synaptic transmission access distinct types of NMDA receptors. Stimulation of glutamatergic afferents to MSNs evoked EPSCs that rely mainly on AMPA receptors because the amplitude of EPSCs was reduced to 22 ± 4% by 2,3-dioxo-6-nitro-1,2,3,4-tetrahydrobenzo[*f*]quinoxaline-7-sulfonamide (NBQX) (30 μM; n = 18). The residual EPSC was abolished by D-AP5 (50 μM; data not shown). This synaptic NMDA current is sensitive to the NR2A/C/D subunit-selective antagonist NVP-AAM077 (0.4 μM; n = 6) (24, 25) and insensitive to the NR2B subunit antagonist ifenprodil (5–10 μM; n = 6; Fig. 3 *A–C*) (26). In contrast, glutamate-dependent gliotransmission is sensitive to NR2B subunit antagonist ifenprodil but insensitive to NVP-AAM077. In six MSNs displaying SIC activity, SICs amplitude was reversibly decreased to 40 ± 15% of control values by ifenprodil (5–10 μM; Fig. 3*D*). In contrast, in six cells NVP-AAM077 did not decrease the amplitude of SICs (0.4 μM; Fig. 3*E*). These results show that astrocytic Ca^{2+} oscillations induce NMDA receptor-dependent SICs in MSNs, which are mediated by NR2B-containing NMDA receptors, a distinct population from synaptic NMDA

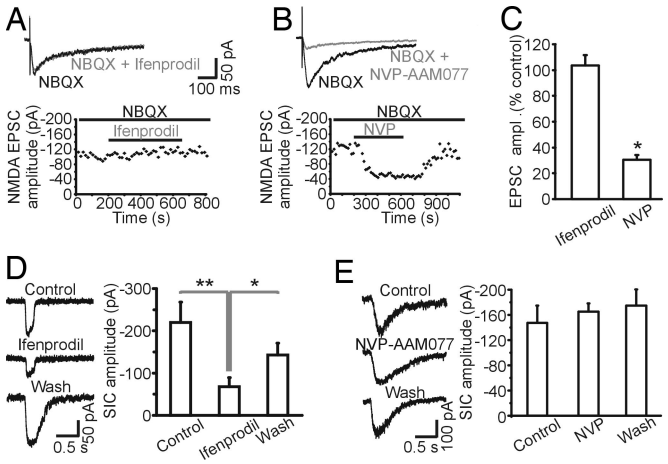

Fig. 3. NR2B-containing NMDA receptors are the preferential target of astrocytic glutamate. (*A*) Ifenprodil (5/10 μM) does not reduce the NMDA EPSC amplitude [averages of 10 excitatory postsynaptic potentials (EPSPs) in each condition]. Experiments performed in the presence of NBQX (30 μM) and 0 Mg^{2+}. (*B*) NR2A antagonist NVP-AAM077 (0.4 μM) reduces NMDA receptor-mediated EPSC amplitude. (*C*) Average amplitude of the NMDA EPSCs in the presence of ifenprodil (n = 6 cells) and NVP-AAM077 (n = 6 cells). Data are normalized to NMDA EPSC amplitude before antagonist application. (*D*) Ifenprodil (5–10 μM) reduces SIC amplitude. (*E*) NR2A antagonist NVP-AAM077 (0.4 μM) does not affect SIC amplitude.

receptors that, based on sensitivity to NVP-AAM077 (24, 25) and their rapid decay kinetics (27) (SI Table 2), indicate that they are mediated by NR1/NR2A-containing NMDA receptors.

Glutamategic Afferents Activate mGluR5-Dependent Gliotransmission. In light of the critical role of mGluR5 for mediating actions of drugs of abuse (4–6), we determined the relative roles of this receptor in regulating synaptic transmission and gliotransmission in the NAc. We stimulated glutamatergic afferents that innervate the NAc while monitoring excitatory postsynaptic potentials (EPSPs) and SICs, respectively. DHPG did not change the strength of synaptic transmission. In both field (n = 6; Fig. 4*A*) and whole-cell (n = 6) recordings (Fig. 4*B*) DHPG had no effect on the field EPSP and EPSC, respectively.

Stimulation of glutamatergic afferents initiated Ca^{2+} oscillations in astrocytes (Fig. 4 *C* and *D*) and significantly increased the frequency of SICs in 9 of 21 MSNs tested (Fig. 4 *E* and *F*). (Afferents were stimulated with 10 trains of stimuli repeated at 1-s intervals. Individual trains consisted of seven stimuli at 30 Hz.) Stimulation of glutamatergic afferents evoked Ca^{2+} oscillations in astrocytes that persisted for several minutes after the stimulus (Fig. 4*C*) and were judged to be due to neuronal activity because TTX (1 μM) blocked stimulus-induced Ca^{2+} oscillations (Fig. 4*D*). Addition of the mGluR5 antagonist MPEP (50 μM) reversibly reduced the activity-dependent induction of astrocytic Ca^{2+} oscillations consistent with afferent activity acting through mGluR5 to stimulate astrocytes (Fig. 4*D*). Similar to Ca^{2+} oscillations, SICs were detected for minutes after afferent stimulation (Fig. 4 *E* and *F*). Blockade of mGluR5 with MPEP (50 μM) prevented the ability of afferent stimulation to induce SICs (Fig. 4*G*). The suppressive effect of MPEP on gliotransmission was not due to a reduction in postsynaptic sensitivity to released glutamate because low Ca^{2+} ACSF, which elevates astrocytic Ca^{2+} independent of mGluRs (23), was still able to stimulate SICs in the presence of MPEP (data not shown). Taken together with the observation that DHPG elevates astrocytic Ca^{2+} and induces SICs, these data demonstrate that mGluR5 is responsible for stimulating gliotransmission in response to afferent stimulation.

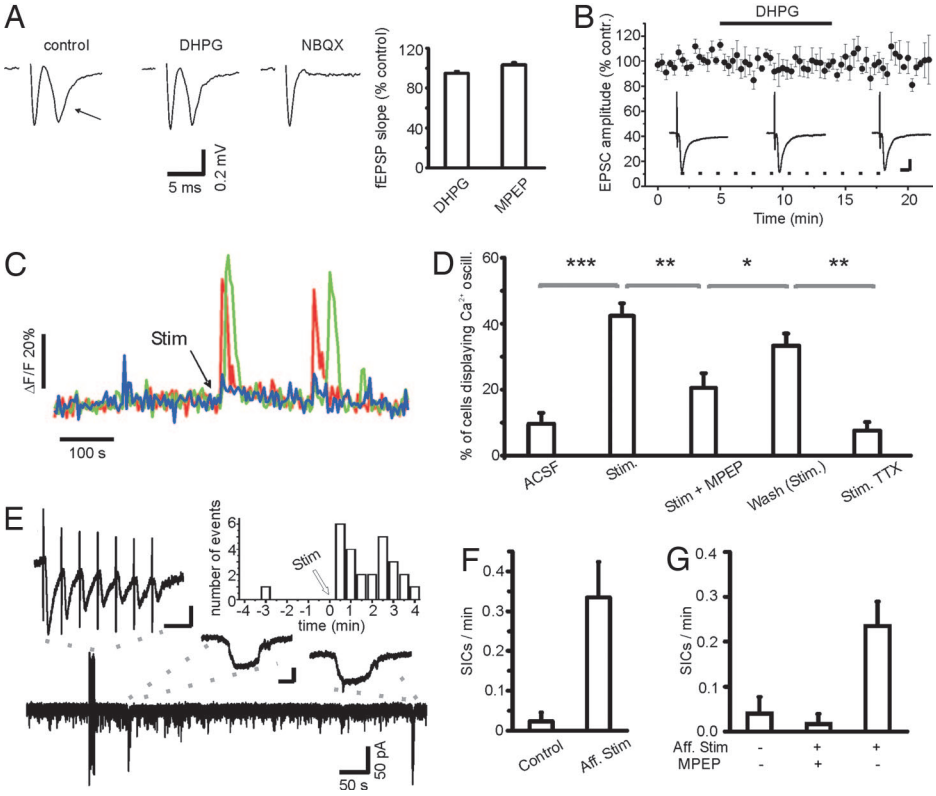

Fig. 4. Glutamatergic afferents activate mGluR5-dependent gliotransmission. (*A*) mGluR5 receptors do not modulate glutamatergic synaptic transmission. (*A Left*) Field EPSPs under control conditions, in the presence of DHPG (20 μM) and NBQX (30 μM). The arrow indicates the EPSP. (*A Right*) Average slope of field EPSPs in the presence of MPEP (50 μM) and DHPG (20 μM) ($n = 6$ slices). (*B*) Whole-cell recording showing that EPSC amplitude is not affected by DHPG application ($n = 6$ cells). (*C*) Astrocyte responses (time course of the $\Delta F/F$ ratio) to glutamatergic afferent stimulation. Afferents were stimulated by using 10 trains of seven stimuli delivered at 30 Hz. (*D*) Average percentage of astrocytes displaying Ca^{2+} oscillations during the sequential experimental conditions ($n = 5$): glutamatergic afferent stimulation, in ACSF, MPEP (50 μM), after washout of MPEP, and in the presence of TTX (1 μM). (*E*) Whole-cell recordings in Mg^{2+}-free ACSF showing two SICs triggered by stimulus trains (10 trains of seven stimuli delivered at 30 Hz) applied to the glutamatergic afferents. See *Inset* for one train of seven stimuli at an expanded time scale. (Scale bar: 50 ms, 50 pA.) Note that stimulation of glutamatergic afferent elicits a prolonged increase in SIC frequency. (*F*) Average SIC frequency in a 3-min time period before and after glutamatergic afferent stimulation ($n = 9$ cells). (*G*) Blockade of mGluR5 by MPEP prevents the ability of glutamatergic afferent stimulation to trigger SICs (MPEP 50 μM, $n = 5$).

Enhanced Gliotransmission at Up-State Membrane Potentials Evokes Increased Action Potential Firing. Because glutamate-dependent gliotransmission selectively activates NMDA receptors, it is important to determine the impact of this signaling pathway on MSNs under physiological concentrations of Mg^{2+} and at membrane potentials normally exhibited by MSNs. The MSNs of the NAc exhibit up- and down-states *in vivo* that are characterized by bistable states in which the membrane potential switches between approximately -85 and -65 mV (28–30). Because the Mg^{2+} block of NMDA receptors can be reduced by depolarization, we asked whether depolarized membrane potentials equivalent to the up-state will enhance glutamate-dependent gliotransmission. In 1 mM Mg^{2+}-containing ACSF and in the presence of TTX, to block activity-dependent synaptic transmission, we recorded the frequency of SICs in MSNs at holding potentials of -85 and -65 mV. Depolarization from -85 to -65 mV increased the amplitude of SICs from -42.0 ± 7.1 to -73.7 ± 12.4 pA ($n = 19$; Fig. 5 *A* and *B*). Coincident with this increased amplitude of SICs at up-state membrane potentials was an increased frequency of detected SICs (Fig. 5*C*) that probably results from an increased sensitivity to detect SICs rather than to a true change in their frequency. In contrast to the enhancement of SIC amplitude at up-state compared with down-state membrane potentials, the amplitude of evoked AMPA/NMDA EPSCs decreased with depolarization (Fig. 5 *D* and *E*) because of a reduced driving force for the AMPA component of the EPSC, although the NMDA EPSC increased similar to NMDA-mediated SICs (Fig. 5 *D* and *E*).

Because SIC but not EPSC amplitude is enhanced with depolarization from -85 to -65 mV, gliotransmission has the potential to provide a powerful excitation to MSNs at up-state membrane potentials. We therefore determined the impact of these SICs on MSN excitability. Afferents were stimulated (10 trains of 7, 30-Hz stimuli; Fig. 5*F*) to evoke delayed astrocytic Ca^{2+} oscillations and gliotransmission while making whole-cell recordings from pairs of MSNs in 1 mM Mg^{2+}-containing ACSF (Fig. 5*F*). One neuron was maintained in voltage-clamp to identify SICs while the paired neuron was maintained in current-clamp to determine the impact of SICs on neuronal activity (Fig. 5*F*). D-AP5 (50 μM) prevented the detection of delayed slow depolarizations and associated SICs ($n = 7$). At a membrane potential of approximately -65 mV, 46% of gliotransmission-evoked depolarizations stimulated action potentials with an average of 15.0 ± 5.6 action potentials per event ($n = 6$; Fig. 5 *F* and *I*). In contrast, at a membrane potential of approximately -85 mV, 38.4% of these astrocyte-dependent depolarizations evoked action potentials (3.0 ± 1.1 action potentials per event, $n = 5$; Fig. 5 *G* and *I*).

Discussion

Given the importance of mGluR5 in mediating self-administration of cocaine and locomotor activity (4–6), it is essential that an understanding of the mechanisms of mGluR5 signaling is identified. We show that the activation of mGluR5 in the NAc activates Ca^{2+} oscillations in astrocytes that lead to the Ca^{2+}-dependent release of glutamate from these glia. This glial-derived glutamate selectively activates NR2B-containing neuronal NMDA receptors of MSNs. Direct excitation of MSNs by afferents is not acutely modulated by mGluR5, although other reports have shown the potential to induce synaptic plasticity (31). Instead, glutamate released from these glutamatergic afferents is responsible for inducing mGluR5-dependent gliotransmission. Thus, activity of afferents has two mechanisms for MSN excitation: direct synaptic activation, and an indirect pathway mediated by mGluR5 and gliotransmission.

Of particular interest is the prolonged activation of gliotransmission by afferent activity. A brief train of stimuli delivered to the afferents evoked astrocytic Ca^{2+} oscillations and gliotransmission for several minutes (Fig. 4*C*). A prolonged response of astrocytes to a brief stimulus has been reported previously. In hippocampal slices, repeated application of the mGluR agonist, trans-ACPD, leads to a prolonged enhancement in Ca^{2+} oscillation frequency in response to subsequent challenges with this agonist (32). Stimulation of the Schaffer collaterals induces gliotransmission detected in

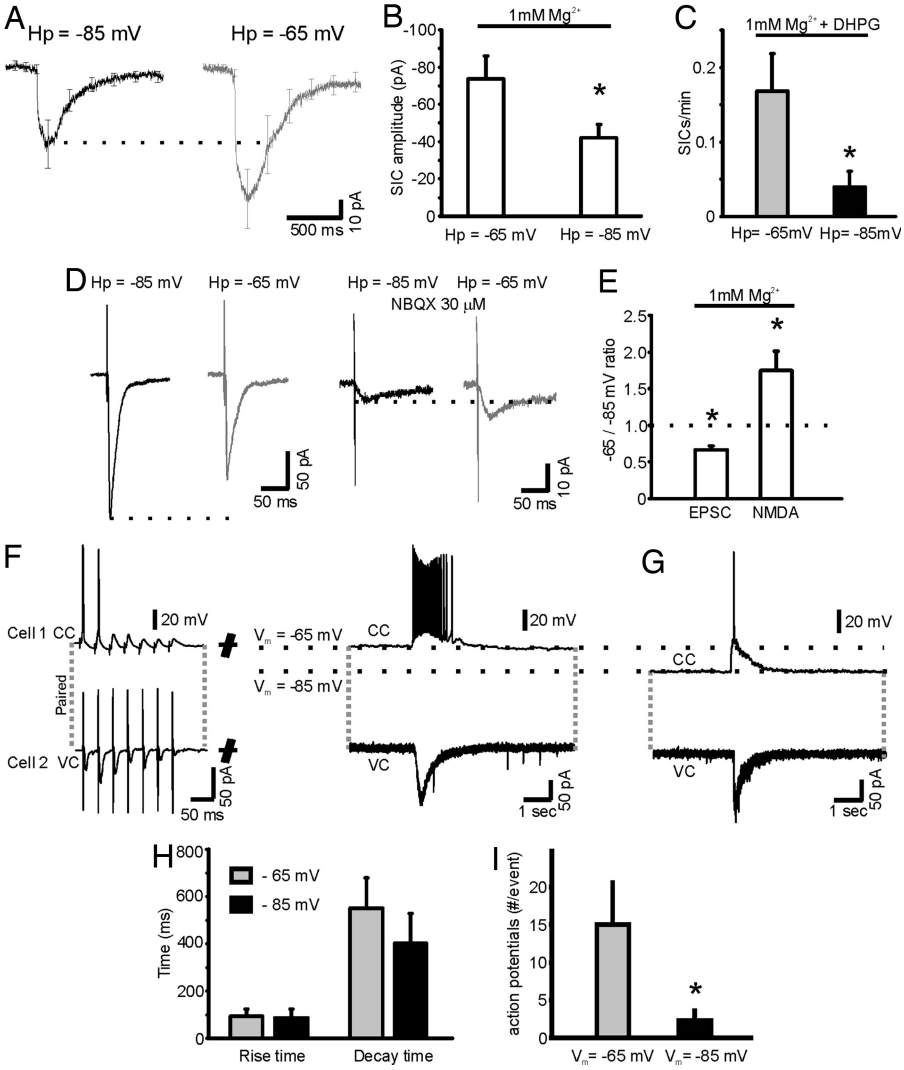

Fig. 5. Gliotransmission drives increased action potential generation in MSNs at up-state membrane potentials. (*A*) Average traces of SICs ($n = 19$) at holding potentials of −85 and −65 mV showing the enhancement of SIC amplitude at up-state (−65 mV) compared with down-state (−85 mV) membrane potentials (error bars are SEM). All experiments reported in this figure were made in 1 mM Mg^{2+}-containing ACSF. (*B*) Average amplitude of the SICs at the two different holding potentials. (*C*) Average SIC frequency after stimulation of class I mGluRs with DHPG (20 μM) at V_h of −85 and −65 mV ($n = 10$). (*D*) The EPSC (*Left*) and pure NMDA-mediated EPSC (*Right*) at holding potentials of −85 and −65 mV. NMDA currents were recorded in NBQX (30 μM). Note the reduction of EPSC amplitude at up-state (−65 mV) compared with down-state (−85 mV) membrane potentials in contrast to the augmentation of the SIC (*A*). Traces in *D* are averages of 10 evoked EPSCs. (*E*) −65/−85 mV ratio of amplitude the EPSC and pure NMDA-mediated EPSC currents at the two different voltages ($n = 5$). (*F*) Paired whole-cell recordings from two closely spaced MSNs in Mg^{2+}-containing ACSF. Glutamatergic afferents were stimulated with 10 trains of seven 30-Hz stimuli (one train shown) that evoked EPSPs in the neuron recorded in current-clamp (*Upper*) and EPSCs in the voltage-clamped neuron (*Lower*). With a delay after afferent stimulation, synchronous excitation of paired MSNs show that gliotransmission powerfully excites MSNs to generate a burst of action potentials. (*G*) In contrast, gliotransmission evokes few action potentials when MSNs are at down-state membrane potentials. (*H*) Comparison on the kinetics of SICs at up- and down-state membrane potentials ($n = 13$ events). (*I*) Average number of action potentials during gliotransmission-mediated depolarization (black bars, $n = 6$; gray bars, $n = 5$).

CA1 pyramidal neurons that can be detected for minutes after the stimulus (15). Chemically induced epileptiform activity increases astrocytic Ca^{2+} oscillation frequency and gliotransmission that lasts for minutes after the termination of neuronal activity by TTX (33). In the NAc, such persistent activation of gliotransmission has the potential to provide long-lasting changes in MSN excitability.

Glutamate-Dependent Gliotransmission Excites GABAergic Neurons. Our results show that, by generating SICs, gliotransmission excites GABAergic neurons. Previous studies performed in the thalamus (34), cortex, and hippocampus (15, 19, 33) have shown that Ca^{2+} elevations in astrocytes lead to the Ca^{2+}-dependent release of glutamate that cause NMDA receptor-mediated currents in glutamatergic neurons. By performing this study in the NAc, where ≈90–95% of the neuronal population is composed of MSNs (35, 36), a class of GABAergic cell, we have been able to demonstrate that glutamate-dependent gliotransmission is a general property of the CNS, and that gliotransmission excites both glutamatergic and GABAergic neurons.

Gliotransmission Acts Preferentially on NR2B-Containing NMDA Receptors. In the NAc, the properties of gliotransmission are similar to those reported in other regions of the CNS. Glial-dependent SICs exhibit many properties that distinguish them from glutamate-dependent synaptic currents: slow kinetics, and insensitivity to TTX and 6-cyano-2,3-dihydroxy-7-nitro-quinoxaline disodium salt (CNQX). Previous studies in the hippocampus using ifenprodil suggested an extrasynaptic target action for glial-derived glutamate (15). In this study, we have evaluated this possibility using antagonists that act on NR2B subunit-containing NMDA receptors and NR2A-containing receptors. Because we see distinct pharmacological sensitivity of afferent synaptic transmission and gliotransmission, we can conclude that gliotransmission acts preferentially on NR2B-containing NMDA receptors presumably located at extrasynaptic sites. Whether gliotransmission affects other extrasynaptic receptors is unknown at this time. This is of particular interest because glutamate arising from a cysteine-glutamate exchanger is known to access extrasynaptic mGluR2/3 (37). Ca^{2+}-regulated glutamate-dependent gliotransmission is a general property of the nervous system that is present in distinct brain regions, including the thalamus (34), area CA1 and CA3 of the hippocampus (15, 33), cortex, and olfactory bulb (33, 38), and the NAc. Gliotransmission is mediated through extrasynaptic NMDA receptors of glutamatergic (15) and GABAergic neurons.

Gating Gliotransmission. In the NAc, MSNs exhibit up- and down-states in which the membrane potential oscillates between approximately −85 and −65 mV (30). Because the Mg^{2+} block of the NMDA receptor is membrane potential-dependent, we asked whether depolarized membrane potentials associated with up-

states would, by removing the Mg^{2+} block of the NMDA receptor, enhance the detection of SICs. We detected SICs with a higher frequency at this depolarized membrane potential (Fig. 5), suggesting that the up-state will gate glutamate-dependent gliotransmission and provide the opportunity for this excitatory pathway to regulate neuronal excitability. Indeed, it is clear that NMDA receptors provide the opportunity for supralinear amplification (39, 40) and that NMDA receptors are required to boost the excitability of MSN neurons (30). In a combined electrophysiology and modeling study, a synaptic NMDA/AMPA receptor ratio of 50%, based on values measured in pyramidal neurons, was used to show the importance of the synaptic NMDA receptor in contributing to neuronal excitability (30). Given that our measurements show the actual ratio to be only 22%, it is possible that the NR2B-containing NMDA receptors activated by gliotransmission contribute to this process of up-state amplification.

Gliotransmission and CREB Phosphorylation. Because the extrasynaptic NMDA receptor density is lower than the synaptic receptor density (41), it is likely that the majority of glial-induced NMDA receptor responses have gone undetected by our recordings and that their main role is not to regulate membrane potential (42). Although we observe gliotransmission-induced NMDA receptor-mediated currents in MSNs, it is likely that an important action of this receptor is in mediating biochemical signaling within the target neuron rather than membrane potential changes *per se*. Several lines of evidence suggest that NMDA receptors may produce diverse outcomes depending on their subunit composition. Whereas the NR2A-containing NMDA receptors stimulate phosphorylation of CREB that drives transcription, activation of NR2B-containing receptors leads to CREB dephosphorylation (43) and to opposing actions. In the NAc, CREB phosphorylation has a particularly critical role in mediating the behavioral response to drug abuse (44). Recent work demonstrated that the increased NAc MSNs excitability caused by CREB helped to limit behavioral sensitivity to cocaine (45). Because glial-derived glutamate acts preferentially through extrasynaptic NR2B-containing NMDA receptors that have been shown to lead to dephosphorylation of CREB (43), it is possible that this mGluR5-induced gliotransmission maintains or enhances responses to drugs of abuse.

In conclusion, we demonstrate that mGluR5 triggers astrocytic Ca^{2+} oscillations and, as a consequence, gliotransmission. Stimulation of glutamatergic afferents, a major excitatory pathway that innervates the NAc, induces persistent gliotransmission that activates NR2B-containing NMDA receptors of MSNs located presumably at extrasynaptic sites. Because stimulation of mGluR5 triggers gliotransmission with no effect on synaptic transmission, our results raise the potential for the involvement of gliotransmission in mediating aspects of mGluR5-dependent drug-induced behaviors.

Materials and Methods

Slice Preparation. All procedures were in accordance with the *Guide for the Care and Use of Laboratory Animals* (National Institutes of Health) and were approved by the University of Pennsylvania's institutional animal care and use committee. Coronal and sagittal slices containing the NAc (250–400 μm) from 2- to 6-week-old C57BL/6 and FVB/NJ mice were prepared (46). Experiments presented in SI Fig. 7 were performed on 9- to 14-day-old pups. After cervical dislocation, the brain was rapidly removed and put in an ice-cold cutting solution containing 120 mM NaCl, 3.2 mM KCl, 1 mM KH_2PO_4, 26 mM $NaHCO_3$, 2 mM $MgCl_2$, 1 mM $CaCl_2$, 10 mM glucose, 2 mM Na-pyruvate, and 0.6 mM ascorbic acid (pH 7.4, 95% O_2/5% CO_2).

Electrophysiology. Slices were continuously perfused with normal ACSF [120 mM NaCl/3.2 mM KCl/1 mM KH_2PO_4/26 mM $NaHCO_3$/1 mM $MgCl_2$/2 mM $CaCl_2$/10 mM glucose (pH 7.4, 95% O_2/5% CO_2, 32°C)]. Intrapipette solution contained 145 mM K-gluconate, 2 mM $MgCl_2$, 5 mM EGTA, 2 mM Na_2ATP, 0.2 mM NaGTP, and 10 mM Hepes (pH 7.2 with KOH). Pipette resistance was 3–4 MΩ. The pipette tip liquid junction potential (−15 mV) was added to all voltages to obtain the correct value of the membrane potential. Recordings were performed from the core region of the NAc. A bipolar tungsten electrode (Warner Instruments, Hamden, CT) was positioned 200–300 μm rostral to the recording electrode and was used to stimulate excitatory afferents at 0.05–0.1 Hz. Inward currents with a rise time of >10 ms, a decay time of >50 ms, and an amplitude of >10 pA were classified as SICs as described (15). Rise time of both SICs and EPSCs was calculated by using a 20–80% criterion, and the amplitude was measured at the peak. The decay time was calculated as the time constant of a single or double exponential fit. Data are expressed as mean ± SEM.

We thank Dr. Julie Blendy for comments on the manuscript, the Haydon laboratory for discussions, and Drs. H. Takano and J.-Y. Sul for assistance with microscopy. This work was supported by the Epilepsy Foundation (T.F.) and National Institutes of Health Grants R37NS037585, R01NS043142, P30NS047321, and P20MH071705 (all to P.G.H.) and NS046478, NS048045, and NS051195 (all to S.J.M.).

1. Kalivas PW (2004) *Curr Opin Pharmacol* 4:23–29.
2. Wolf ME (1998) *Prog Neurobiol* 54:679–720.
3. Vanderschuren LJ, Kalivas PW (2000) *Psychopharmacology (Berlin)* 151:99–120.
4. Chiamulera C, Epping-Jordan MP, Zocchi A, Marcon C, Cottiny C, Tacconi S, Corsi M, Orzi F, Conquet F (2001) *Nat Neurosci* 4:873–874.
5. Tessari M, Pilla M, Andreoli M, Hutcheson DM, Heidbreder CA (2004) *Eur J Pharmacol* 499:121–133.
6. Backstrom P, Hyytia P (2006) *Neuropsychopharmacology* 31:778–786.
7. Popik P, Wrobel M (2002) *Neuropharmacology* 43:1210–1217.
8. Aoki T, Narita M, Shibasaki M, Suzuki T (2004) *Eur J Neurosci* 20:1633–1638.
9. Haydon PG (2001) *Nat Rev Neurosci* 2:185–193.
10. Volterra A, Meldolesi J (2005) *Nat Rev Neurosci* 6:626–640.
11. Volterra A, Magistretti PJ, Haydon PG (2002) *The Tripartite Synapse: Glia in Synaptic Transmission* (Oxford Univ Press, Oxford).
12. Pascual O, Casper KB, Kubera C, Zhang J, Revilla-Sanchez R, Sul JY, Takano H, Moss SJ, McCarthy K, Haydon PG (2005) *Science* 310:113–116.
13. Cai Z, Schools GP, Kimelberg HK (2000) *Glia* 29:70–80.
14. van den Pol AN, Romano C, Ghosh P (1995) *J Comp Neurol* 362:134–150.
15. Fellin T, Pascual O, Gobbo S, Pozzan T, Haydon PG, Carmignoto G (2004) *Neuron* 43:729–743.
16. Nestler EJ (2005) *Nat Neurosci* 8:1445–1449.
17. Wise RA (1996) *Curr Opin Neurobiol* 6:243–251.
18. Angulo MC, Kozlov AS, Charpak S, Audinat E (2004) *J Neurosci* 24:6920–6927.
19. Perea G, Araque A (2005) *J Neurosci* 25:2192–2203.
20. Zhuo L, Sun B, Zhang CL, Fine A, Chiu SY, Messing A (1997) *Dev Biol* 187:36–42.
21. Matthias K, Kirchhoff F, Seifert G, Huttmann K, Matyash M, Kettenmann H, Steinhauser C (2003) *J Neurosci* 23:1750–1758.
22. Wallraff A, Odermatt B, Willecke K, Steinhauser C (2004) *Glia* 48:36–43.
23. Zanotti S, Charles A (1997) *J Neurochem* 69:594–602.
24. Auberson YP, Allgeier H, Bischoff S, Lingenhoehl K, Moretti R, Schmutz M (2002) *Bioorg Med Chem Lett* 12:1099–1102.
25. Neyton J, Paoletti P (2006) *J Neurosci* 26:1331–1333.
26. Williams K (1993) *Mol Pharmacol* 44:851–859.
27. Vicini S, Wang JF, Li JH, Zhu WJ, Wang YH, Luo JH, Wolfe BB, Grayson DR (1998) *J Neurophysiol* 79:555–566.
28. O'Donnell P, Greene J, Pabello N, Lewis BL, Grace AA (1999) *Ann NY Acad Sci* 877:157–175.
29. Goto Y, O'Donnell P (2001) *J Neurosci* 21:4498–4504.
30. Wolf JA, Moyer JT, Lazarewicz MT, Contreras D, Benoit-Marand M, O'Donnell P, Finkel LH (2005) *J Neurosci* 25:9080–9095.
31. Robbe D, Alonso G, Manzoni OJ (2003) *Ann NY Acad Sci* 1003:212–225.
32. Pasti L, Volterra A, Pozzan T, Carmignoto G (1997) *J Neurosci* 17:7817–7830.
33. Fellin T, Gomez-Gonzalo M, Gobbo S, Carmignoto G, Haydon PG (2006) *J Neurosci* 26:9312–9322.
34. Parri HR, Gould TM, Crunelli V (2001) *Nat Neurosci* 4:803–812.
35. Kawaguchi Y, Wilson CJ, Augood SJ, Emson PC (1995) *Trends Neurosci* 18:527–535.
36. Meredith GE (1999) *Ann NY Acad Sci* 877:140–156.
37. Moran MM, McFarland K, Melendez RI, Kalivas PW, Seamans JK (2005) *J Neurosci* 25:6389–6393.
38. Kozlov AS, Angulo MC, Audinat E, Charpak S (2006) *Proc Natl Acad Sci USA* 103:10058–10063.
39. Schiller J, Schiller Y (2001) *Curr Opin Neurobiol* 11:343–348.
40. Schiller J, Major G, Koester HJ, Schiller Y (2000) *Nature* 404:285–289.
41. Noguchi J, Matsuzaki M, Ellis-Davies GC, Kasai H (2005) *Neuron* 46:609–622.
42. Haydon PG, Carmignoto G (2006) *Physiol Rev* 86:1009–1031.
43. Hardingham GE, Fukunaga Y, Bading H (2002) *Nat Neurosci* 5:405–414.
44. Carlezon WA, Jr, Duman RS, Nestler EJ (2005) *Trends Neurosci* 28:436–445.
45. Dong Y, Green T, Saal D, Marie H, Neve R, Nestler EJ, Malenka RC (2006) *Nat Neurosci* 9:475–477.
46. Nicola SM, Malenka RC (1998) *J Neurophysiol* 79:1768–1776.